Canadian Science Publishing

ARTICLE

Tidal erosion and upstream sediment trapping modulate records of land-use change in a formerly glaciated New England estuary

Justin L. Shawler, Christopher J. Hein, Elizabeth A. Canuel, James M. Kaste, Gregory G. Fitzsimons, Ioannis Y. Georgiou, and Debra A. Willard

Abstract: Land clearing, river impoundments, and other human modifications to the upland landscape and within estuarine systems can drive coastal change at local to regional scales. However, as compared with mid-latitude coasts, the impacts of human modifications along sediment-starved formerly glaciated coastal landscapes are relatively understudied. To address this gap, we present a late-Holocene record of changing sediment accumulation rates and sediment sources from sediment cores collected across a tidal flat in the Merrimack River estuary (Mass., USA). We pair sedimentology, geochronology, bulk- and stable-isotope organic geochemistry, and hydrodynamic simulations with historical data to evaluate human and natural impacts on coastal sediment fluxes. During the 17th to 19th centuries, accumulation rates increased by an order of magnitude in the central tidal flat, likely in response to enhanced delivery of terrestrial sediment resulting from upland deforestation. However, the overall increase in accumulation (0.56–2.6 mm/year) within the estuary is subtle and spatially variable across the tidal flats because of coincident anthropogenic land clearing and dam building, upland sediment storage, and estuarine hydrodynamics. This study provides insight into the response of formerly glaciated fluvial-coastal systems to human modifications, and underscores the role of estuarine environmental conditions in modifying upland signals of land-use change.

Key words: land-use change, sediment accumulation, estuarine dynamics, tidal flats, sediment source, Merrimack River estuary.

1. Introduction

Land-use change can dramatically impact the transport and deposition of sediments to and along the coast. The arrival of European-style agriculture to North America and subsequent deforestation increased sediment loads to the affected coastal zones through an estimated tenfold increase in soil-erosion rates (Meade 1982). In the United States, sediments derived from land clearing by the first European settlers resulted in the rapid

Received 3 January 2019. Accepted 24 July 2019.

J.L. Shawler. Virginia Institute of Marine Science, William & Mary, P.O. Box 1346, Gloucester Point, VA 23062, USA; Department of Geology, William & Mary, P.O. Box 8795, Williamsburg, VA 23185, USA.
C.J. Hein and E.A. Canuel. Virginia Institute of Marine Science, William & Mary, P.O. Box 1346, Gloucester Point, VA 23062, USA.
J.M. Kaste. Department of Geology, William & Mary, P.O. Box 8795, Williamsburg, VA 23185, USA.
G.G. Fitzsimons. GGF Historical Consultants, Lowell, MA, USA.
I.Y. Georgiou. Department of Earth and Environmental Sciences, University of New Orleans, New Orleans, LA 70148, USA.
D.A. Willard. U.S. Geological Survey, 926A National Center, Reston, VA 20192, USA.
Corresponding author: J.L. Shawler (e-mail: jshawler@vims.edu).

progradation of estuarine bayhead deltas in the Chesapeake Bay in Maryland (Pasternack et al. 2001) and the Roanoke River in North Carolina (Jalowska et al. 2015). In North Carolina, late 20th century tree farming in the Newport River watershed led to rapid accretion in the associated estuary and eventual marsh progradation (Mattheus et al. 2009). Along the Missouri and Mississippi rivers, sediment discharge during peak agricultural land use resulted in a 220% increase in the wetland area of the Mississippi River Delta between 1838 Common Era (CE) and 1932 CE (Tweel and Turner 2012).

Despite the robust body of literature documenting the effects of humans on sediment transport from uplands to the coastal zone, there is insufficient understanding of anthropogenic effects on sediment fluxes from paraglacial landscapes; that is, those which retain geomorphic features and sediments that were derived directly or indirectly from glacial processes (Forbes and Syvitski 1994). In such settings, glacial processes have removed and reworked surficial sediment and altered sediment transport pathways. Recent efforts to understand the effects of deforestation on sediment transport on these landscapes offer contradictory interpretations. Kirwan et al. (2011) concluded that increased coastal sediment accumulation from land-clearing during the 17th and 18th centuries increased lateral marsh growth near the Parker and Rowley rivers in northeast coastal Massachusetts (USA). However, Priestas et al. (2012) argued that these findings were inconsistent with evidence from historical maps and questioned the dating methods. Along some parts of paraglacial coastal Maine (USA), low landscape gradients restrict the export of sediments from logging sites to local watersheds (Kasprak et al. 2013), mitigating any potential increase in coastal sediment delivery from deforestation. Additional features of the paraglacial landscape, such as armored soils and large lakes and bogs that interrupt many glaciated fluvial systems, reduce the modern sediment loads of New England rivers (Meade 1982). This scenario is further complicated by the fact that paraglacial coastal landscapes were formed during periods of enhanced fluvial sediment discharge associated with meltwater from retreating ice sheets, but today a combination of natural (e.g., depletion of glacial deposits) and anthropogenic (e.g., stabilized slopes, river dams) conditions have greatly reduced river sediment discharges (Hein et al. 2014). Whereas short-term records from the last ca. 30 years link declining fluvial suspended sediment concentrations to the presence of dams along rivers in New England (Weston 2014), the centennial-scale effects of damming and land-use change (particularly within larger drainage basins) on sediment delivery from paraglacial landscapes, such as New England, remain largely unknown.

As with studies of terrestrial sediment export, investigations of local anthropogenic and natural impacts on sedimentation records and processes within estuaries have also often focused on sediment-rich coastal plain settings (e.g., Tambroni and Seminara 2006; Mattheus et al. 2009; Elliott et al. 2015). However, extensive local anthropogenic changes also occurred in paraglacial estuaries during the historical period. Indeed, recent research attributes increased sediment trapping in off-river waterbodies along the paraglacial Connecticut River (USA) to anthropogenic maintenance of tidal inlets and tie-channels (Woodruff et al. 2013). Paraglacial estuarine systems without off-river waterbodies can provide sedimentary records of anthropogenic disturbances to estuarine health and water quality (e.g., Hartwell 1970; Hubeny et al. 2018). However, less is known about the potential for paraglacial estuaries to preserve records of past sediment fluxes. In the absence of estuarine settling basins and off-river waterbodies, tidal flats and fringing saltmarshes are the primary depocenters of upland-derived sediments in estuaries (e.g., Hartwell 1970; Meade 1982). Yet, tidal flats are subject to natural processes, such as tidal channel meandering (Fruergaard et al. 2011) and equilibrium morphodynamics (Fagherazzi et al. 2006), that may eliminate their sedimentary records. Additionally, marshes often provide poor records of sediment provenance because of the high rates at which they produce autochthonous

organic matter, overprinting organic-matter-based source signatures of allochthonous sediments (e.g., Saintilan et al. 2013).

Refining the relative role of distal and proximal natural and anthropogenic activities in shaping coastal sediment delivery in paraglacial settings is particularly important in light of the threatened state of associated saltmarshes due to low inputs of fine-grained minerogenic sediments (Carey et al. 2017; Watson et al. 2017*a*, 2017*b*). Here, we use a transect of sediment cores collected across a mesotidal, river-mouth tidal flat to document late-Holocene changes in sediment provenance and fluxes to an estuary along the formerly glaciated New England coast. We pair historical evidence with geochronology provided by radiocarbon, pollen, and sediment geochemistry to document the combined effects of natural processes and both regional and local anthropogenic activities on estuarine tidal flat sediment accumulation rates. Additionally, we use our transect design to explore spatial and temporal changes in sediment source inferred from grain size and stable isotope organic geochemistry. We investigate the role of factors such as coincident upper-watershed land clearing and lower-watershed dam building, the equilibrium morphodynamics of tidal flats, and the potential for terrestrial sediment storage in controlling sediment delivery to, and record preservation in, paraglacial estuaries.

2. Site description and land use history

2.1. Physical setting

The Merrimack River (Fig. 1) is the fourth largest river by drainage area in New England, with a watershed that drains the formerly glaciated landscape of New Hampshire and northern Massachusetts. The Merrimack River is bordered by sandy glacial deposits and weathered granitic plutons (FitzGerald et al. 2005; Hein et al. 2014). Sandy proglacial sediments were derived primarily from physically and chemically weathered granites, with sediments eroded and reworked through the advance and retreat of Wisconsinan (ca. 75–11 ka) and Illinoian (ca. 191–139 ka) glaciers (Hanson and Caldwell 1989; Stone et al. 2006). Modern estuarine channels of the Merrimack River transport sub-angular to rounded quartzose sands with abundant feldspar, mica, and rock fragments (>30%), indicative of granitic origin and local, glacigenic source (FitzGerald et al. 2005).

The Merrimack River is tidal up to 35 km from its mouth in the western Gulf of Maine. The lower 5 km is characterized by a wide embayment where fringing marsh and tidal flats, including the 5800 m^2 Joppa Flats (Fig. 1), occupy shallow depths (between −1.5 and +1.5 m local mean sea level (MSL)). The average depth of the river channel in the lower estuary is 2.5 to 10 m below MSL and average width is 200 to 500 m. At its mouth, the Merrimack River inlet is restricted by two jetties and bounded to the north and south by barrier islands: Salisbury Beach and Plum Island, respectively.

The Merrimack River estuary is a relatively shallow, strongly forced, salt-wedge estuary (Ralston et al. 2010). Mean tidal range is 2.5 m and spring tidal range is 4.0 m. The tidal cycle and river discharge control water mixing in the highly stratified estuary (Ralston et al. 2010). The Merrimack River estuary water column is weakly stratified during low-discharge periods, but during high-discharge events — particularly during flooding tides — the water column becomes highly stratified, with internal shear mixing occurring during the early ebb, and boundary layer mixing at the end of the ebb tide (Ralston et al. 2010). Bedload transport primarily occurs during high-discharge events associated with spring freshets and tropical and extratropical storms (FitzGerald et al. 2005).

2.2. Regional and local land-use history

Anthropogenic impacts in the Merrimack River watershed include deforestation, dredging, river damming, industrialization, and urbanization (Fig. 2). Extensive land clearing in

Fig. 1. Study site and core locations. (*a*) Regional map of the Gulf of Maine in the northeastern United States of America (USA). (*b*) Merrimack River watershed (blue), which has its headwaters in the White Mountains (New Hampshire, USA). Black symbols indicate the locations of major river dams in the watershed. (*c*) The Merrimack River estuary is located northwest of Plum Island, Massachusetts. Prominent flow constrictions, other anthropogenic influences (e.g., jetties, harbors, roads, and highways), and sites of interest are noted by arrows. (Imagery: Google, TerraMetrics). (*d*) Satellite image of Joppa Flats tidal flats in the Merrimack River estuary (Google, TerraMetrics), showing current profiler deployment site (square) and core locations (circles) collected along a transect oriented from SSW to NNE. Site A is proximal to the river bank, while site E is proximal to the river channel.

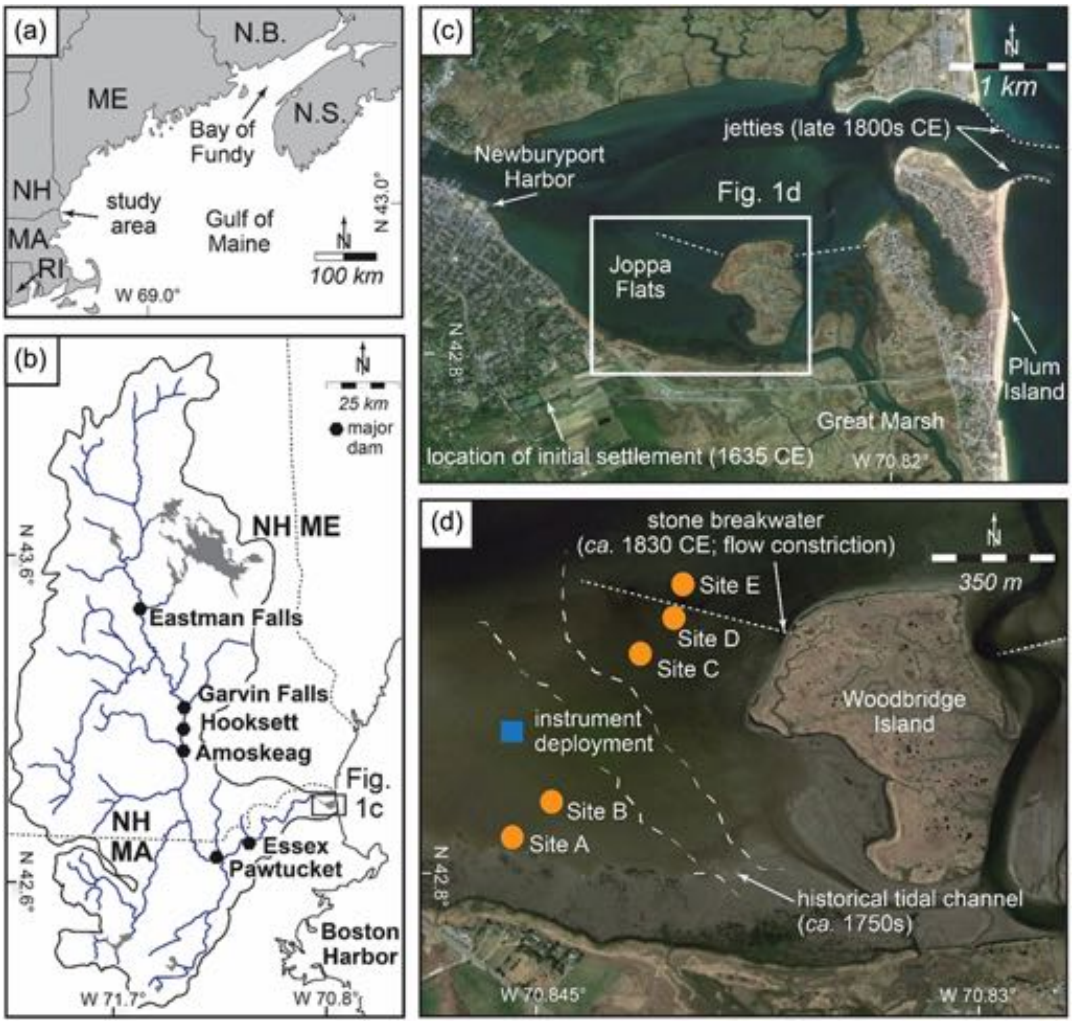

the lower watershed was initiated with the arrival of European colonists and reached its peak in the upper watershed in 1870 CE (U.S. Army Corps of Engineers 1911). Dams for textile mills (Fig. 1*b*) in the Merrimack River watershed date to the 1820s at Lowell and the late 1840s at Lawrence (Molloy 1976; Steinberg 1991), with earlier mills being predominately small grist and sawmill operations (Donahue 2004). Dredging operations for waterway navigation in the Merrimack Valley above Newburyport began during the era of steamboats, around 1870 CE (Bradlee 1920). Additional dredging for improving waterpower potential, primarily for textile mills, occurred after the Civil War; however, most of this work was

Fig. 2. Major anthropogenic events in the Merrimack River (M.R.) watershed. (*a*) Timeline of anthropogenic events during and following European colonization. Initial settlement and land clearing in the lower watershed began in 1635 CE and continued until 1700 CE, while upper watershed peak deforestation and logging occurred between 1844 and 1890 CE, approximately coincident with large-scale industrial damming of the Merrimack River. Late 19th and 20th century modifications include dredging and the installation of hard infrastructure to control the flow of the river. All dates are in years CE and their citing sources can be found in text in Subsect. 2.2. (*b*) Schematic diagram differentiating a natural coupled river-coastal system (left) from a human-modified river-coastal system (right). In the human-modified system, sediment transport pathways and river basin storage mechanisms are controlled by dams and flow constrictions, while urbanization and deforestation dictate upstream sediment fluxes. At the coast, shoreline armoring and the construction of groins and jetties change longshore transport rates and fluxes.

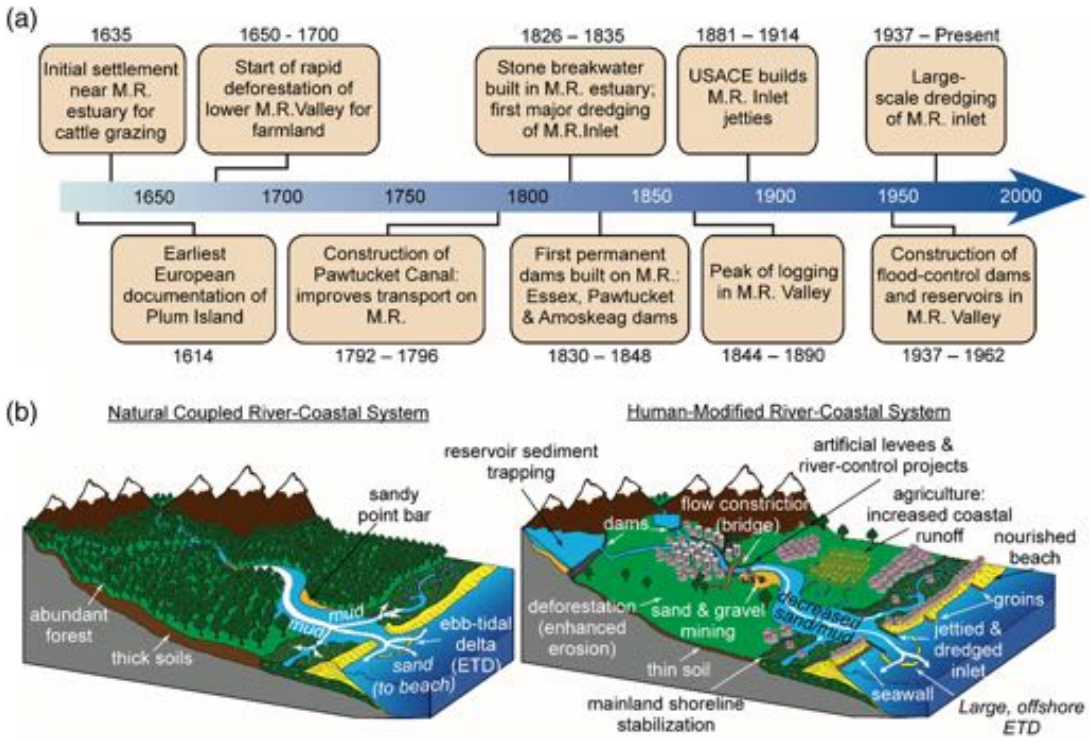

centered around the confluence of the Merrimack and Concord rivers and at Hunt's Falls on the Merrimack (Malone 2009). More recently, this region has undergone considerable urbanization (Mayer et al. 2002). For example, residential construction had started on wetlands and proximal to stream channels in the Merrimack Basin by 1968 (Wood et al. 1970). By the late 20th century, urban and suburban development expanded to include more than 13% of the entire Merrimack River basin (Flanagan et al. 1999).

Localized anthropogenic impacts to the estuary include land clearing from early Colonial settlement to the 19th century followed by hard engineering structures designed to stabilize the inlet and control the flow of the Merrimack River. The first documented European settlement near the estuary began in 1635 CE, at which time nearly 400 acres (~162 ha) of cleared land was used for cattle grazing along the waterside (Currier 1902). The town of Newburyport was officially chartered in 1764 CE, and by the 1790s was among the most prosperous ports in New England (Labaree 1962). Completion of the Plum Island Turnpike (a road) in 1806 CE allowed for easy travel between the town of Newburyport and Plum Island, and initiated development of that barrier island (Fallon et al. 2017).

Completion of an approximately 580 m long stone breakwater (Fig. 1*c*) in the estuary in 1831 CE was an attempt to control the shifting river channel (Smith 1854). An additional 294 metric tons of stone was added to the breakwater in conjunction with the erection of a pier on the northern riverbank (U.S. Army Corps of Engineers 1835). In response to continued navigation issues, the U.S. Army Corps of Engineers constructed a set of stone jetties along the northern and southern banks of the river mouth beginning in 1881 CE and 1883 CE, respectively. Construction and subsequent lengthening of the jetties continued for nearly two decades (Hartwell 1970). River-mouth dredging projects occurred throughout the 20th century and were complemented by jetty repairs in the late 1960s and most recently in 2014 CE (Hein et al. 2019).

3. Methods

3.1. Sample collection

Sediment cores were collected in June 2015 CE using a pontoon-mounted piston-corer, an approach that minimizes artificial compaction. Five sites were chosen along a marsh-edge to river-channel-proximal transect across the estuary to ensure a reliable record from the dynamic tidal flat environment (Fig. 1). Additionally, our sampling scheme allows us to understand how changing wave and tidal energy from the riverbank towards the modern river channel controls preservation of estuarine sedimentary records. Two cores were collected at each site. Cores were each collected in a single drive, and varied in length from approximately 130 to 150 cm. The first core was split horizontally, logged visually and with an Avaatech XRF Core Scanner (see Supplementary Data S.1.4[1]), and subsampled for grain size, palynological analysis, and total organic carbon (TOC) and nitrogen (TN) analyses. The second core was subsampled vertically (1 cm interval) for bulk density, loss-on-ignition, and ^{137}Cs and ^{210}Pb analyses.

3.2. Sediment core stratigraphy

All cores were photographed and described using visual standards for color (Munsell 2000), texture, and mineralogy. Cores from sites A, C, and E were sampled at 1 cm intervals for quantitative grain-size analysis from 0 to 30 cm, and 5 cm intervals thereafter. Grain-size samples were analyzed on a Beckman Coulter LS I3 320 laser diffraction particle size analyzer in the Woods Hole Oceanographic Institution (WHOI) Coastal Systems Group laboratory. A subset of 34 samples selected at random were analyzed in triplicate; resulting standard deviations of grain size were used to calculate an average instrumental uncertainty of ±3%.

3.3. Sediment core chronology and accumulation rates

We constrain sediment core chronology with Δ^{14}C analyses, *Ambrosia* and *Cerealia* pollen abundance data, and short-lived radionuclide concentrations. Eight samples total of mollusk, wood, and organic matter were analyzed for radiocarbon content at the National Ocean Science Accelerator Mass Spectrometry facility at WHOI. All radiocarbon ages were calibrated using OxCal 4.2 (Bronk Ramsey 2009), which includes a reservoir correction. Terrestrial samples (roots, wood, and organic matter) were calibrated with Intcal13 (Reimer et al. 2013) calibration curves. Marine samples (all mollusks) were calibrated using Marine13 (Reimer et al. 2013), corrected to a regionally averaged local reservoir correction (ΔR) of 107 ± 37 years (following Hein et al. 2012).

[1]Supplementary material is available with the article through the journal Web site at http://nrcresearchpress.com/doi/suppl/10.1139/anc-2018-0034.

Pollen and spores in samples from sites A, C, and E were isolated using standard preparation techniques (Willard et al. 2001; Traverse 2007). Samples were washed with HCl and HF to remove carbonates and silicates, respectively, and acetolyzed (1 : 9, sulfuric acid : acetic anhydride) in a boiling bath for 10 min. After neutralization, samples were treated with 10% KOH for 10 min at 70 °C and then neutralized. Residual sample material was sieved at 149 and 5 μm to remove the coarse and fine palynomorph fractions, respectively. When necessary, samples were swirled on a watch glass to remove any additional inorganic material. Samples were then stained with Bismarck Brown and mounted onto slides in glycerin jelly. In general, at least 300 pollen grains and spores were counted from each sample to determine the percent abundance and concentration of palynomorphs, which were generally identified to the genus or family level.

Samples for gamma analysis were oven-dried at 50 °C, homogenized, weighed, packed in either 25 or 12 mL (as determined by available sample volume) Petri dishes, sealed using vinyl electrical tape and paraffin wax, and stored for at least 30 days to ensure equilibrium between ^{226}Ra and its radon daughters ^{214}Pb and ^{214}Bi. The samples were measured for ^{137}Cs (662.6 keV photopeak) and ^{210}Pb (46.5 keV photopeak) activity by gamma spectroscopy using a shielded ultra-low background Canberra 5030 Broad Energy Germanium gamma detector for a period of at least 24 h (see Supplementary Data S.1.2 for uncertainty and calibration[1]). The constant rate of supply (CRS) model (Appleby and Oldfield 1978; Appleby 2001) was applied to calculate age estimates in the upper portion of the cores.

Sedimentation rates were calculated for sites A (bank-proximal) and C (central) using the "classical" age-depth modeling software package Clam 2.1 (Blaauw 2010). Geochronological inputs to the model include the oldest ^{210}Pb CRS age estimate, *Ambrosia* pollen horizon, and calibrated ^{14}C dates. However, because of the inherent uncertainty associated with radiocarbon dating, we use only four radiocarbon dates for determination of sediment accumulation rates.

3.4. Bulk organic carbon and nitrogen analyses

TOC and TN contents, and stable isotope compositions for TOC and TN ($\delta^{13}C_{TOC}$ and $\delta^{15}N_{TN}$) were determined at 5 cm intervals from cores A, C, and E at the WHOI Organic Mass Spectrometry Facility. Prior to analysis, samples were freeze-dried, homogenized, and powdered. Samples for TOC, TN, $\delta^{13}C_{TOC}$, and $\delta^{15}N_{TN}$ were analyzed in triplicate on an elemental analyzer coupled to a Finnegan Deltaplus isotope ratio mass spectrometer. TN and $\delta^{15}N_{TN}$ compositions were measured on raw powdered sample aliquots. TOC and $\delta^{13}C_{TOC}$ were determined following fumigation acidification of powdered sample aliquots (Whiteside et al. 2011). These sample aliquots were sealed in a vacuum desiccator with a beaker of 50 mL 12N HCl, fumigated for 60 to 72 h at 60–65 °C to remove carbonates, and dried in a separate desiccator for an additional 24 h prior to measurement. Bulk sediment TOC and TN are controlled predominantly by sediment texture (Hedges and Keil 1995), and thus values are reported in text and figures following normalization to sample grain size (percentage <63 μm) (see Supplementary Data Fig. S2[1]).

3.5. Hydrodynamics, sediment mobility, and erosion potential

A hydrodynamic model (Delft3D; Lesser et al. 2004) that was previously developed and validated with deployments in Plum Island Sound (Fig. 1*d*) was used to provide time-dependent water level and velocity in the vicinity of the cores to assess sediment mobility in the modern system. Sediment mobility was assessed using a sediment transport model (SEDTRANS05; Neumeier et al. 2008) capable of simulating both cohesive and non-cohesive suspended and bedload transport for multiple size classes (for model details, see Neumeier et al. 2008). The model was applied as a "point model", in that tide-dependent conditions

Fig. 3. Stratigraphic cross section of Joppa Flats tidal flat. Site A is located proximal to the modern riverbank and marsh, and site E is proximal to the river channel. Primary stratigraphic horizons and relations are denoted by dashed lines. Note the channel fill deposits at depth in the cores proximal to the modern marsh and the organic-rich deposits at depth in the cores proximal to the modern river. Core elevations are relative to local mean sea level (MSL).

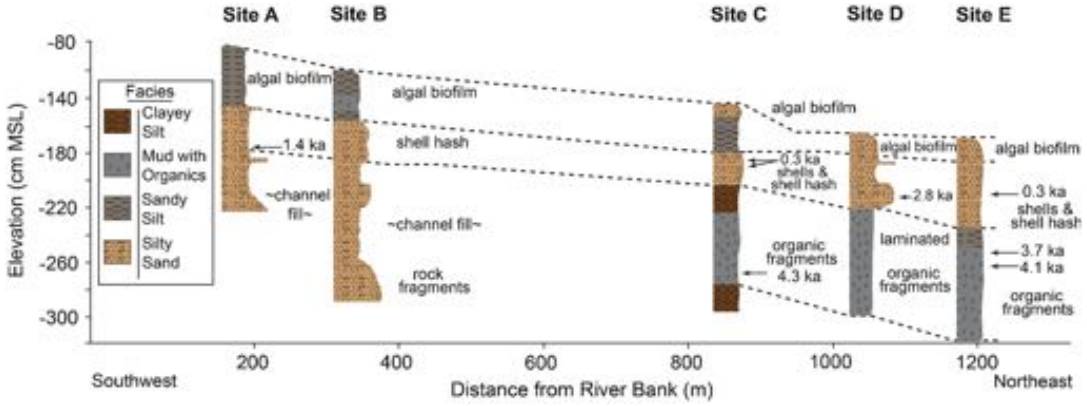

were simulated at one location (not spatially across the flats) where water level and tidal velocities were collected (Fig. 1*d*). The model was driven with the depth-integrated velocity. The sediment model was initialized with grain-size data from sediment cores for sand (average D_{50} (~115 μm) from the upper 10 cm of sites A (60 μm), C (134 μm), and E (154 μm)) and used literature values to set critical erosion stress for cohesive transport (e.g., 0.5–0.7 Pa; Fagherazzi et al. 2006; Xu et al. 2015). Other inputs to the model included roughness height selected based on the grain diameter of sand (bed was free of bedforms), settling velocities for each sediment class (Stokes settling), and sediment density for sand (2650 kg/m^3) and mud (1600 kg/m^3).

4. Results

4.1. Joppa flats stratigraphy

Sites A, C, and E are predominantly composed of silt (3.9–63 μm) and sand (>63 μm), with the clay (<3.9 μm) fraction ranging from 0.9% to 6.0%. Sediment textures are spatially variable at depths greater than approximately 60 cm from the sediment surface: river-proximal sites (cores C, D, and E) are marked by a relatively organic-rich (average TOC: 3.4% ± 0.2 percentage points) bed that extends laterally for at least 400 m, whereas bank-proximal sites (cores A and B) are characterized by fining-upward deposits interpreted as channel fill (Fig. 3). Sediments at site A progressively fine upward, with the sand fraction decreasing from an average of 69% ± 10 percentage points at 120–35 cm to 38% ± 7 percentage points in the upper 35 cm of the core (Fig. 4). The bottommost sections of core B contain pebble-sized rock fragments. All cores contain a layer of coarse sand and shell hash from approximately −150 to −210 cm MSL. The uppermost ~30 cm of each core contains silty sand (sand <50% ± 3 percentage points), but this unit coarsens in the upper 10–20 cm at sites C, D, and E (sand >70%), which are proximal to the modern channel of the Merrimack River. Sediments at sites C and E generally coarsen upward. Core C has a sandier unit (sand >65% ± 3 percentage points) from 60–40 cm below the sediment surface (Fig. 5). Core E, the most river-proximal, contains sand with minor silt (average sand content of 77% ± 3 percentage points) in the upper 85 cm (Fig. 6). In all cores, a layer of algal biofilm was present in the topmost 5 to 10 cm.

Fig. 4. Sedimentology and bulk organic and stable isotope stratigraphy of site A. (*a*) Lithology and down-core profiles of (*b*) grain size, grain-size-normalized weight-percent (*c*) total organic carbon ($\overline{TOC}$), and (*d*) total nitrogen ($\overline{TN}$) contents, and stable isotopic composition of bulk organic (*e*) carbon ($\delta^{13}C_{TOC}$) and (*f*) nitrogen ($\delta^{15}N_{TN}$). (*g*) Chronology derived from stratigraphic marker horizons.

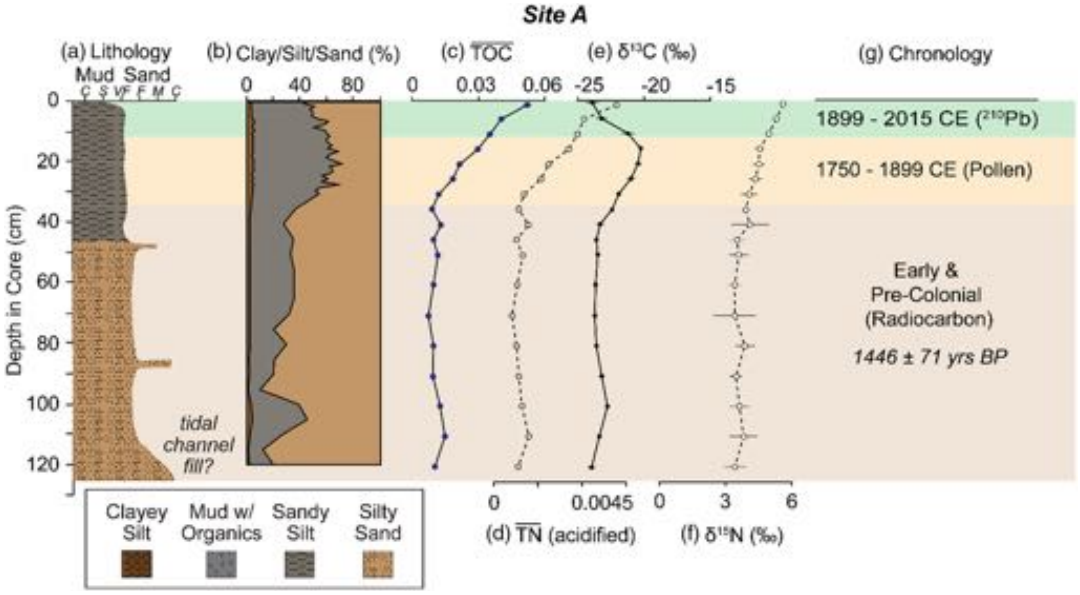

Fig. 5. Sedimentology and bulk organic and stable isotope stratigraphy of site C. (*a*) Lithology and down-core profiles of (*b*) grain size, grain-size-normalized weight-percent (*c*) total organic carbon ($\overline{TOC}$) and (*d*) total nitrogen ($\overline{TN}$) contents, and stable isotopic composition of bulk organic (*e*) carbon ($\delta^{13}C_{TOC}$) and (*f*) nitrogen ($\delta^{15}N_{TN}$). (*g*) Chronology derived from stratigraphic marker horizons.

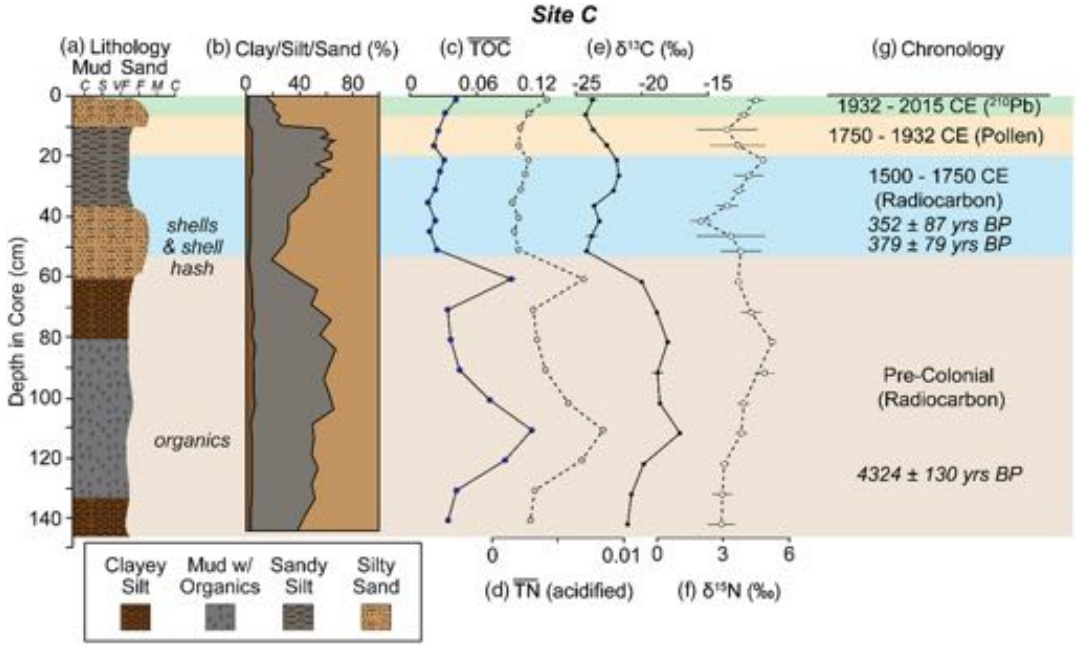

Fig. 6. Sedimentology and bulk organic and stable isotope stratigraphy of site E. (*a*) Lithology and down-core profiles of (*b*) grain size, grain-size-normalized weight-percent (*c*) total organic carbon ($\overline{TOC}$) and (*d*) total nitrogen ($\overline{TN}$) contents, and stable isotopic composition of bulk organic (*e*) carbon ($\delta^{13}C_{TOC}$) and (*f*) nitrogen ($\delta^{15}N_{TN}$). (*g*) Chronology derived from stratigraphic marker horizons.

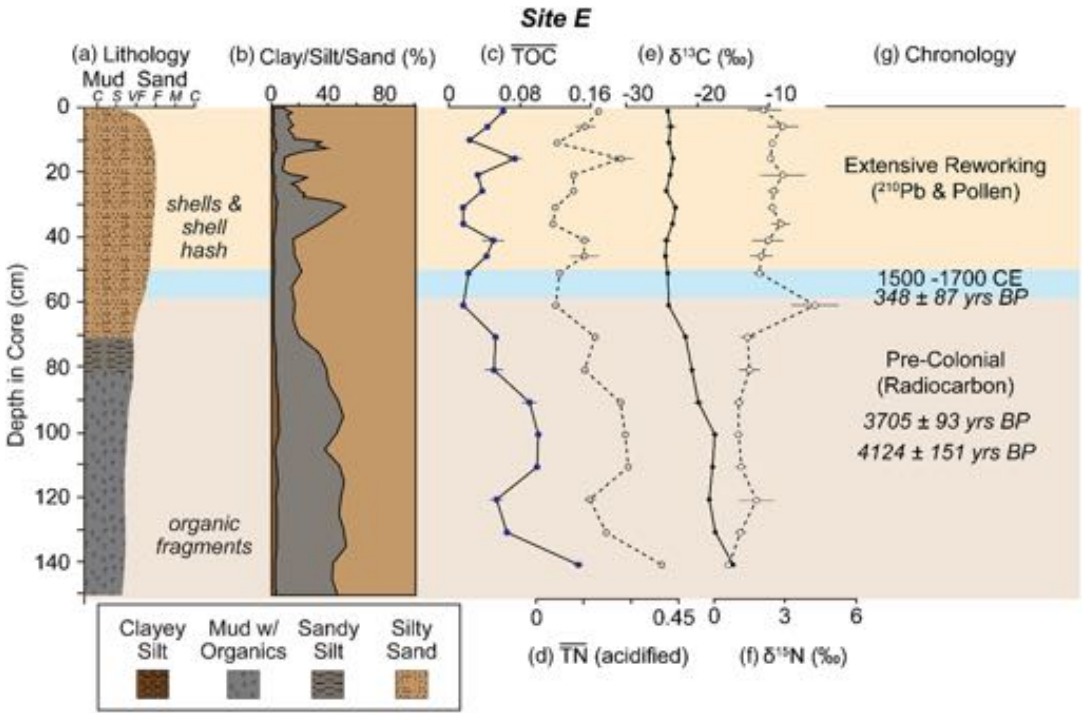

4.2. Joppa flats sediment geochronology

4.2.1. Evidence of localized reworking at bank- and channel-proximal sites

Total ^{210}Pb measurements from sites A (bank-proximal) and C (central) exceed supported ^{210}Pb values at and above 11.5 and 6.5 cm, respectively (Fig. 7). These sites both contain typical diffusion-like ^{137}Cs profiles, wherein activities generally decrease downcore following surface maxima. CRS accumulation histories were determined for sites A (bank-proximal) and C (central) from 1899 CE ± 36 years and 1932 CE ± 12 years, respectively, to 2015 CE. At site E (river-proximal), both total ^{210}Pb and ^{137}Cs activities vary throughout the upper 20 cm; data from this site do not meet the assumptions of the CRS model. Site E (river-proximal) is situated within the highest-energy region of the transect, ca. 300–400 m from the modern river channel. The relatively dilute and mixed ^{210}Pb, ^{137}Cs, and pollen-abundance data observed in the upper 50 cm of the core (Fig. 6) reflect the high degree of reworking anticipated at such exposed locations (see Andersen et al. 2000). Analysis of site E topo-bathy LIDAR data (U.S. Army Corps of Engineers 2018) indicates localized scour around gaps in the nearby stone breakwater (built ca. 1830 CE), and enhanced deposition at and adjacent to site E (river-proximal) (see Supplementary Data Fig. S3[1]). For these reasons, data from site E (river-proximal) are not used for sedimentation records. Likewise, the base of core A (bank-proximal) presents complex stratigraphy (i.e., paired fining-upward sequences interpreted as channel infilling) indicative of punctuated deposition prior to 1446 ± 71 cal. years BP (Fig. 4). For this reason, geochronological interpretations from site A (bank-proximal) are restricted to the upper ~90 cm.

Fig. 7. Chronostratigraphic proxy data from sites A, C, and E. (*a*) Downcore profiles of palynomorph abundance of *Ambrosia* (open circles with dashed lines) and *Cerealia* (closed circles with solid lines). Plots in rows (*b*) and (*c*) show activities of total and supported ^{210}Pb and ^{137}Cs, respectively. (*d*) The constant rate of supply (CRS) age model was applied to derive accumulation histories for sites A and C. Site E did not meet the assumptions of the CRS model, because of our interpretation of reworking of the upper approx. 50 cm of the profile.

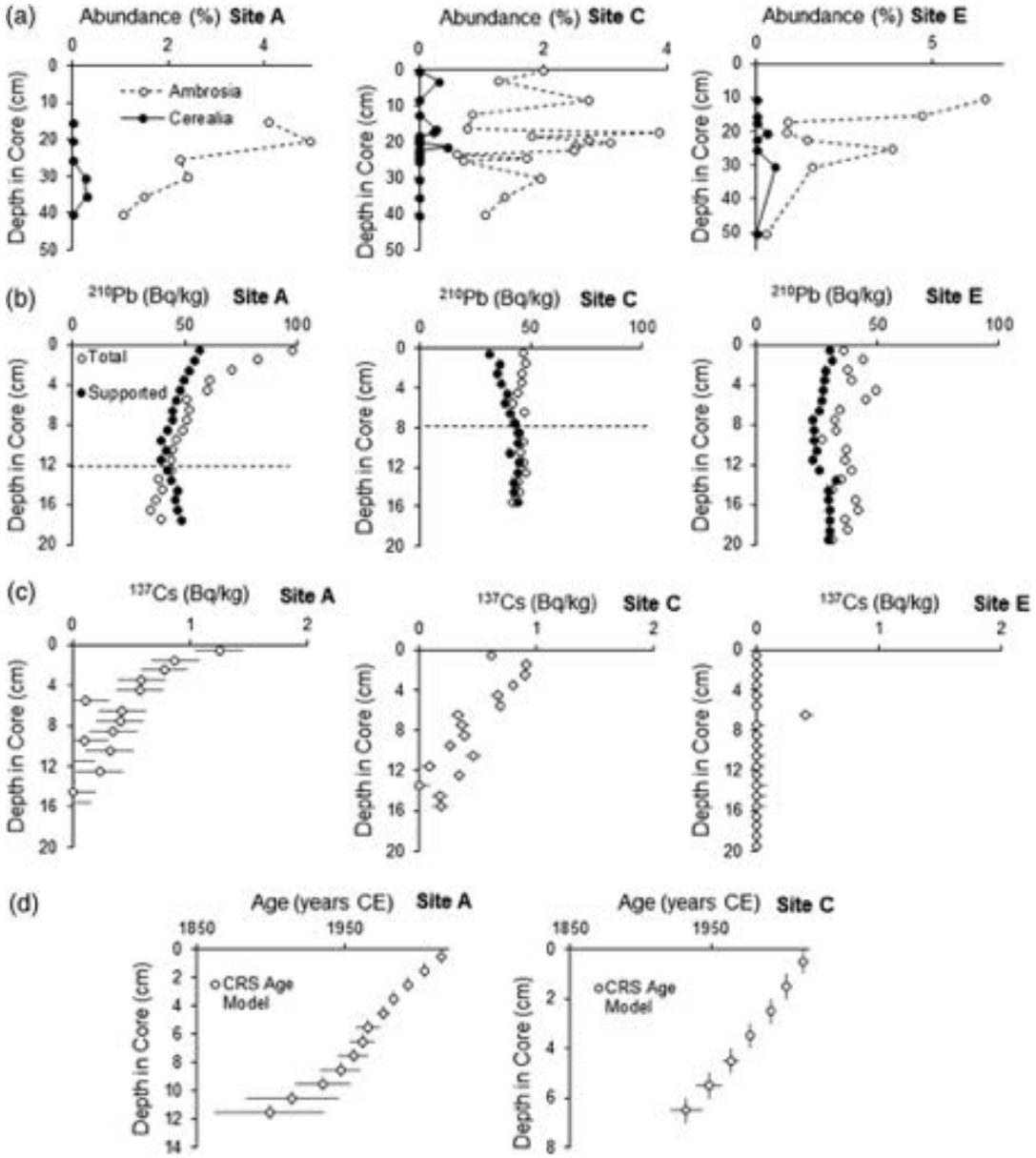

4.2.2. Pre-European and European horizon at central and bank-proximal sites

The contact between Joppa Flats sediment deposited before and after initial European settlement is constrained by radiocarbon and palynological data from sites A (bank-proximal) and C (central). Three radiocarbon dates (Table 1) from site C (4324 ± 130 cal. years BP (pre-Colonial); 379 ± 79 cal. years BP (ca. 1571 CE); 352 ± 87 cal. years BP (ca. 1598 CE))

Table 1. Radiocarbon data.

Core	NOSAMS accession number	Latitude (°N)	Longitude (°W)	Dated material	Depth in core (cm)	Elevation (m MSL)	$\delta^{13}C$ (‰ VPDB)	Reported age (years BP)	Cal. 2σ age (years BP)
Site A	OS-127553	42.80147	70.84605	Root	83–87	−1.76 ± 0.02	Not measured	1550 ± 25	1446 ± 71[a]
Site C	OS-121278	42.80696	70.84238	*Mya arenaria*	44–51	−1.825 ± 0.035	1.25	810 ± 20	352 ± 87[a]
Site C	OS-121808	42.80696	70.84238	Wood	52–56	−1.89 ± 0.02	−24.82	340 ± 15	379 ± 79[a]
Site C	OS-122934	42.80696	70.84238	Wood	132–133	−2.675 ± 0.035	−28.31	3890 ± 45	4324 ± 130[a]
Site D	OS-122935	42.80830	70.84122	Salt peat	61–62	−2.105 ± 0.005	−17.39	2750 ± 35	2838 ± 81
Site E	OS-121279	42.80935	70.84097	Shell fragment	53–60	−2.115 ± 0.0035	1.32	805 ± 20	348 ± 87
Site E	OS-121807	42.80935	70.84097	Wood	98–100	−2.54 ± 0.02	−26.64	3450 ± 20	3705 ± 93
Site E	OS-122933	42.80935	70.84097	Salt peat	108–109	−2.635 ± 0.005	−15.32	3760 ± 45	4124 ± 151

Note: All radiocarbon ages were calibrated using OxCal 4.2 (Bronk Ramsey 2009), which includes a reservoir correction. Terrestrial samples (peat, roots, and wood) were calibrated with Intcal13 (Reimer et al. 2013) calibration curves. Marine samples (all mollusks) were calibrated using Marine13 (Reimer et al. 2013), corrected to a regionally averaged ΔR of 107 ± 37 years. All dates in text and table are reported as 2σ calibrated ages before 1950.

[a]Sample used for accumulation rate calculation.

identify the location of the upper boundary of pre-Colonial sediment to between 44 and 56 cm depth. We assumed that all terrestrial material (e.g., wood) for radiocarbon dating was rapidly reworked and transported to and deposited in the estuary. Recognizing the limitations of such assumptions, we further constrain post-Colonial deposition ages with pollen data. The transition from early Colonial sediment accumulation to the start of widespread land clearing at site C (central) is marked by pollen assemblages of >2% *Ambrosia* and the presence of *Cerealia* between a core depth of 21 and 23 cm. At site A the agricultural horizon is located between 35.5 cm (*Cerealia*) and 30.5 cm (>2% *Ambrosia*) depth. For coastal New England, the agricultural horizon has been interpreted as 1629 CE in Salem, Mass. (Hubeny et al. 2018), and as late as 1785 CE along the Gulf of Maine coast (Ward et al. 2008). The lower Merrimack River was first settled in the 1630s CE, grist and sawmills developed on smaller local rivers by 1645 CE (Currier 1902), and extensive settlement and a busy commercial harbor occupied the adjacent waterside by the 1760s CE (Labaree 1962). Therefore, a date of 1700 CE ± 50 years is assigned to this horizon at sites A (bank-proximal) and C (central). Additionally, an increase in abundance (>4%) of *Ambrosia* between 15 and 20 cm depth in site A (bank-proximal) likely represents the early peak of upper watershed deforestation between 1820 and 1880 CE (see Foster 1992).

4.2.3. 20th century horizon at central and bank-proximal sites

We use the ^{210}Pb horizon to differentiate sediment accumulation during the Colonial Era and Industrial Revolution (17th to late 19th century) from that which occurred during the 20th century. The diffusion-type ^{137}Cs profiles may result from bioturbation, similar to profiles that were observed in cores from Salem Sound, Mass. (~35 km south of Joppa Flats; Hubeny et al. 2018) or leaching of ^{137}Cs, which has been observed in deepwater lakes in New England and Scandinavia (Davis et al. 1984). However, the ^{210}Pb and ^{137}Cs radioisotope horizons are internally consistent, and found at ~6.5 cm below the surface at site C (central) and ~11.5 cm below the surface at site A (bank-proximal). Furthermore, these horizons are consistent with total Pb elemental abundance values determined from X-ray fluorescence (see Supplementary Data section S.2.4 and Fig. S4[1]). The latter provide a secondary marker horizon that is coincident with the onset of nationwide industrial lead production (late 19th century) and the introduction of leaded gasoline in automobiles (mid- to late-20th century) in the U.S. (Kemp et al. 2012).

4.3. Sediment accumulation and mobility

The overall low accumulation rates (0.2–2.8 mm/year; Fig. 8) and sand-dominated sediment observed in all cores are consistent with the low total suspended solids (9.0–15.0 mg/L) measured in the Merrimack River in this study during the spring 2014 freshet (Supplemental Table S4[1]). During the 17th to 19th centuries, sediment accumulation within Joppa Flats increased by an order of magnitude, but rates remained moderate (maximum: 2.8 mm/year) even then.

Low accumulation rates may reflect the high degree of sediment mobility within Joppa Flats: during the ~18 day period simulated in Delft3D, Joppa Flats was submerged approximately 74% of the time, during which period sediment mobility was present for at least 25% of the time. Near-bed velocity exceeds 0.3 m/s, producing transport in the direction of flow (Fig. 9), for approximately 2 h centered on each tide reversal (approximately four times daily). The resulting water transport direction, and thus sand transport direction, exhibits some asymmetry (primary azimuth NW-N and SE) and, as such, produces net transport asymmetry ($\sim 6 \times 10^{-4}$ $m^3 m^{-1} s^{-1}$) toward the northwest–north, in the direction of the upstream Merrimack River.

Fig. 8. Sedimentation rates. Sedimentation rates have been calculated for sites A (*a*) and C (*b*) using the "classical" age-depth modeling software package Clam 2.1 (Blaauw 2010). Geochronological inputs to the model include the oldest ^{210}Pb CRS age estimate, *Ambrosia* pollen horizon, and calibrated ^{14}C dates.

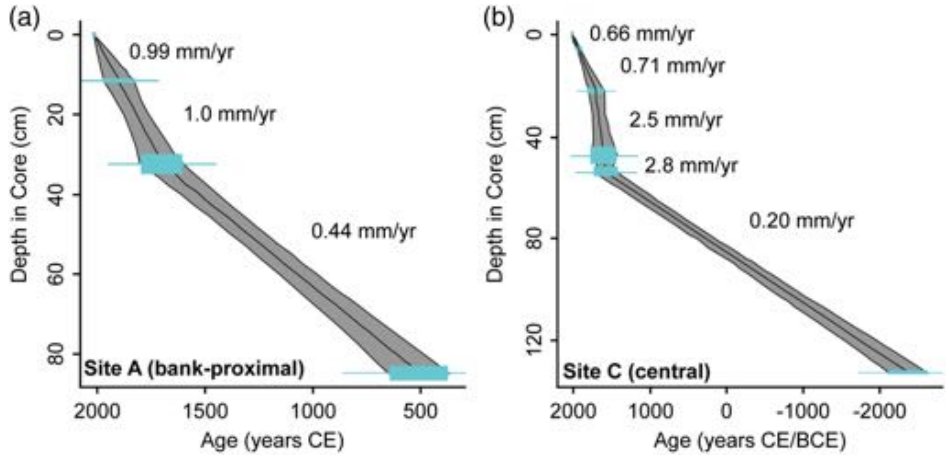

Fig. 9. Water level, velocity, and current direction. (*a*) Simulated water level (gold solid line) and velocity (blue solid line) in Joppa Flats near the core sites. (*b*) Time-dependent vector plot showing depth-averaged current direction. (*c*) Collapse vector plots showing tidal current direction and magnitude over the ~18 day simulation period; the water transport direction exhibits some asymmetry (primary azimuth NW-N and SE).

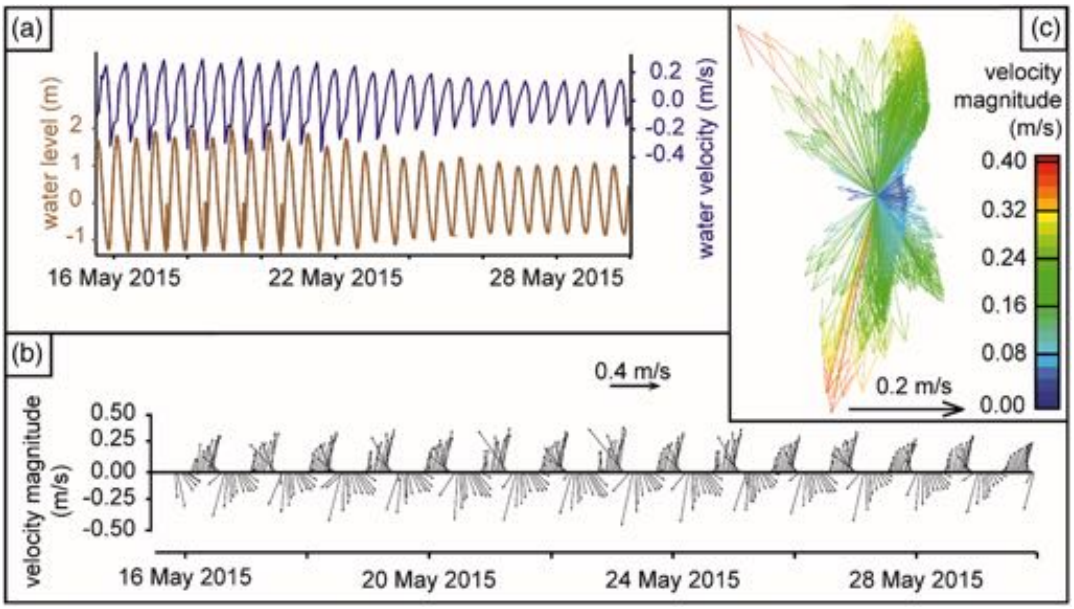

4.4. Sediment sources

$\delta^{13}C_{TOC}$ and C : N values from all core samples indicate a mix of organic matter sources common to estuaries (Cloern et al. 2002; Bianchi and Bauer 2011). Linear regression shows a co-varying relationship between $\delta^{13}C_{TOC}$ and sediment grain size, indicating time-varying contributions of sediment to the estuary from fluvial and estuarine (likely marsh and

Fig. 10. Geochemical and grain-size relationships for sites A and C. (*a* and *b*) Linear regression of sediment samples (differentiated by chronological horizons) reveals co-varying sediment grain size and organic matter source ($\delta^{13}C$) shifts during the late Holocene. (*c* and *d*) Comparison of values of $\delta^{13}C$ and C : N of samples from sediment cores and local rivers and estuaries reveals relative changes in organic-matter source contributions to Joppa Flats over time. Errors are within data points.

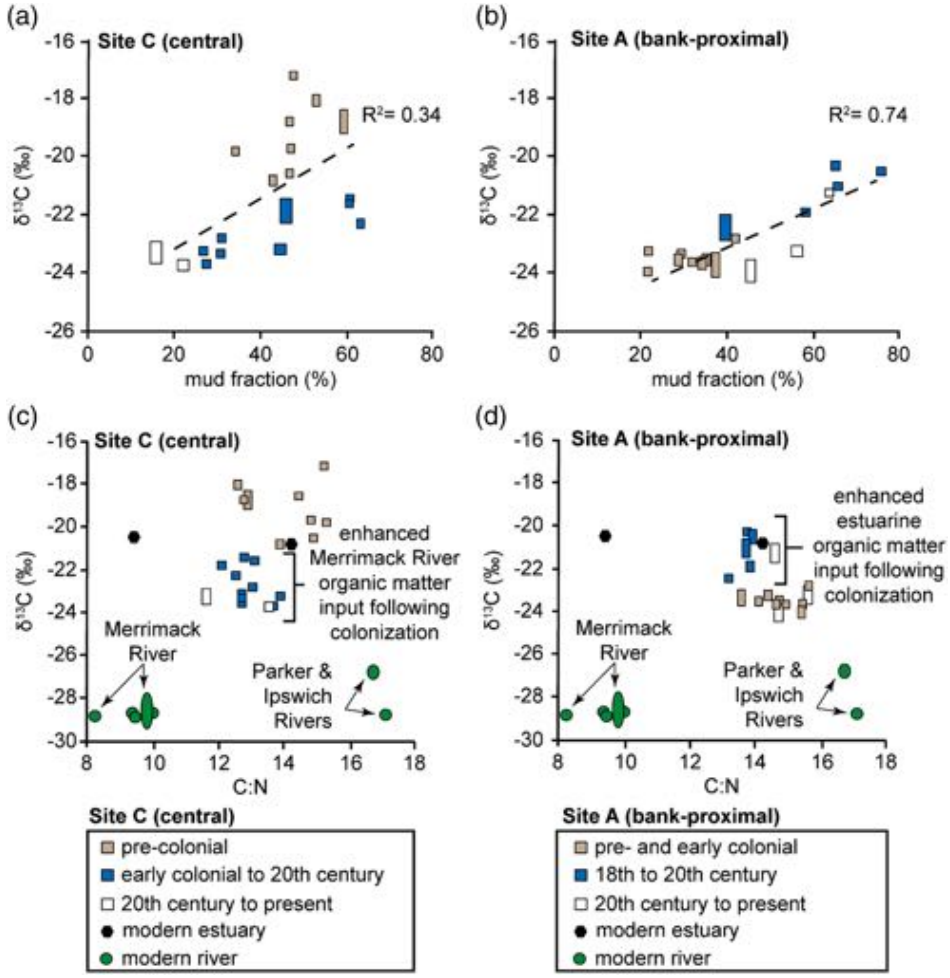

marine) sources (Fig. 10). These source variations are also spatially nonuniform across Joppa Flats. At site A (bank-proximal), sandy sediments (average: 32% ± 6 percentage points mud) with more negative $\delta^{13}C$ values (−23.5‰ ± 0.2 per mille points) accumulated during pre-Colonial and early Colonial periods (until ca. 1750 CE) are gradually replaced by muddier sediments (average: 60% ± 12 percentage points mud) with more positive $\delta^{13}C$ values (−21.2‰ ± 0.2 per mille points) during the 18th to early 20th centuries (Fig. 10). We interpret this shift to reflect an increased contribution of sediment and organic matter from fringing riverbank saltmarshes (literature $\delta^{13}C$ values: −12‰ to −14‰) and marine or estuarine sources (literature $\delta^{13}C$: −18‰ to −24‰ (Fry and Sherr 1984; Currin et al. 1995); local average $\delta^{13}C$: −20.7‰ ± 0.2 per mille points). We observe an opposite shift at site C (central), where muddier sediments (average: 50% ± 7 percentage points mud) with more positive $\delta^{13}C$ values (–19.2‰ ± 0.1 per mille points) are found during pre-Colonial deposition. These are replaced

by sandier sediments (average: 44% ± 14 percentage points) with more negative $\delta^{13}C$ values (average: −22.6‰ ± 0.1 per mille points) during the early Colonial period through the 20th century (Fig. 10), suggesting a mix of both marine or estuarine and terrestrial sediment during this time. This shift toward more negative $\delta^{13}C$ values could reflect increased influence of upland-derived sources via the main Merrimack River channel (average $\delta^{13}C$: −28.7‰ ± 0.1 per mille points), possibly associated with basin-scale land clearing. During the 20th century, sediments (average $\delta^{13}C$ value: −23.1‰ ± 0.4 per mille points) suggestive of mixed terrestrial and (or) marine sources contribute to both locations, though these are muddier (average: 55% ± 8 percentage points) at site A (bank-proximal) and sandier (average: 19% ± 3 percentage points mud) at site C (central).

5. Discussion

5.1. Estuarine sediment accumulation history

Observations of low sediment accumulation rates (0.2–2.8 mm/year) throughout the mid-to-late Holocene in the Merrimack River estuary and low modern total suspended solids (9.0–15.0 mg/L) in the Merrimack River support regional evidence that paraglacial coastal environments of New England are starved of fine-grained inorganic sediment, a feature attributed to the widespread removal of sediments from river basins by glaciers and by dam-building (Meade 1969; Weston 2014). For example, in Plum Island Sound, located immediately to the south of Joppa Flats, fluvial sediment inputs are below global averages and well below the mineral sediment inputs necessary for local marsh accretion to keep pace with relative sea-level rise (Hopkinson et al. 2018). Approximately 35 km south of Joppa Flats, Salem Sound exhibits similarly low sediment accumulation rates (0.12–0.22 cm/year), also attributed to low terrestrial sediment fluxes (Hubeny et al. 2018). Indeed, where higher historical (ca. 19th century to present) sediment accumulation rates are observed in paraglacial estuaries (e.g., Ribble Estuary, United Kingdom: 4–11 mm/year), the cause is attributed to local engineering projects, such as reclamation and channel dredging, rather than regional changes in land use (van der Wal et al. 2002).

Observed sediment accumulation rates at Joppa Flats are generally within a single order of magnitude through time, which limits clear interpretations of changing sediment fluxes, particularly during the post-European settlement period. Subtle changes in sediment accumulation rates, and particularly the increase following colonization (from 0.20–0.44 to 1.0–2.8 mm/year), may reflect natural variability in sediment supply to the estuary. However, higher rates of estuarine sediment accumulation in the central flats during the period of European colonization are consistent with the lateral marsh growth documented locally by Kirwan et al. (2011), as well as subtle sedimentation increases recorded in upland ponds in New England (Francis and Foster 2001) during this same period.

The relative provenance of sediment delivered to the Merrimack Estuary varied during the transition from the pre-Colonial period to the period of increased land clearing during the 17th through 20th centuries. Specifically, the riverbank-proximal tidal flat received greater contributions of muddy sediment from local marsh and estuarine sources, whereas the central tidal flat, where fluvial influence is likely greater, experienced an increase in sandier, likely upland-derived, sediments. The accumulation of mixed-grain sediment with mixed terrestrial and marine influence occurred from ca. 1900 CE to present at both the central and riverbank-proximal regions of the tidal flat and is interpreted to reflect urbanization of the watershed. During the 20th century, residential development increased in the Merrimack River watershed, with these land uses accounting for ~13% of land cover by the late 20th century (Flanagan et al. 1999). Elsewhere, urban and suburban runoff has resulted in coarser-grained sediment accumulation in streams and rivers (e.g., Russell et al. 2018),

which is consistent with the minor coarsening-upward trend observed during the 20th century at both sites A and C (Figs. 4 and 5).

5.2. Proximal human and natural influences on estuarine sediment accumulation

Estuaries are sediment sinks for many U.S. Atlantic Coast rivers, potentially archiving and preserving records of both natural (Elliott et al. 2015) and anthropogenic (Zimmerman and Canuel 2000, 2002; Hubeny et al. 2018) changes in sediment accumulation for millennia (Meade 1982; Slattery and Phillips 2011). However, preservation of these records can be complicated by mixing due to waves, tides, and bioturbation, and sediment deposition may be punctuated in response to tidal-channel formation and closure (Fruergaard et al. 2011). At Joppa Flats, records from site E (river-proximal) and the base of site A (bank-proximal) emphasize the complex local dynamics of moderate-energy tidal environments, such as sediment reworking and tidal-channel migration. Environmental conditions also influence sediment provenance data: proximal to the riverbank (i.e., site A), saltmarsh-derived sediments appear to overwhelm (or mask) any upland-derived sedimentary signal from 17th, 18th, and 19th century land-clearing.

In addition to reworking by these local environmental conditions, we hypothesize that tidal erosion across the flats may explain the overall low sediment accumulation rates in the tidal flat. Observations and modelling indicate that tidal flats maintain an equilibrium elevation relative to mean sea level through competition between deposition and erosion by wind waves (Fagherazzi et al. 2006, 2007; Defina et al. 2007; Hu et al. 2018). Given this potential geomorphic process, and no observed conversion of tidal flats to marshes across Joppa Flats, it is tempting to conclude that any increase in sediment accumulation in the Merrimack River estuary larger than that preserved and recorded here was possibly balanced by erosion, forcing the maintenance of near-equilibrium elevations in the estuary. In addition, the proximity of Joppa Flats to the Merrimack River promotes twice-daily tidal exchange of water with the Merrimack River estuary (Ralston et al. 2010), a process that our sediment transport simulations indicate could further facilitate erosion. Thus, it is possible that local erosive processes balanced some increase in sediment accumulation in Joppa Flats, maintaining near-equilibrium estuary bathymetry and buffering signals of varying sediment fluxes.

Local environmental conditions likely demonstrate a greater control over tidal flat deposition than local engineering works. Specifically, a stone breakwater (built with the intention of controlling the flow of the river in the estuary) and two river-mouth jetties (inlet stabilization) have limited direct influence on sediment accumulation at our sites. For example, the increased prevalence of coarse sediment and mixed marine and terrestrial organic matter influence during the 20th century observed in our sediment cores could be attributed to the effects of increased inlet stabilization and subsequent import of marine sediment. However, sediment transport in the Merrimack River inlet is ebb-dominated (FitzGerald et al. 1994; Hein et al. 2019), which limits fluxes of marine sediment into Joppa Flats. Additionally, data from this study show sediment transport asymmetry from the tidal flats towards the Merrimack River channel, indicating that Joppa Flats receives limited marine deposition; it is thus expected that marine sedimentary signatures in our core records would be relatively muted. Likewise, there is no evidence from our data of impacts from the 19th century stone breakwater. The upper 60–70 cm of both cores D (within the breakwater) and E (outside the breakwater) contain nearly identical grain sizes and coarsening-upward trends, indicative of similar current and wind-wave energy regimes throughout their depositional history despite the presence of the stone breakwater beginning in ca. 1831 CE. Furthermore, hydrodynamic and sediment-transport data from this study demonstrate that the central Joppa Flats, despite being located within the portion of the tidal flats "sheltered"

by the breakwater, experience currents strong enough to mobilize sediment, indicating minimal effects of the stone breakwater on sediment accumulation.

5.3. Distal human and natural influences on estuarine sediment accumulation

Natural sediment trapping upstream of the estuary may also limit sediment fluxes from the terrestrial landscape to the coast. While research across latitudes highlights the important role of sediment storage within floodplains (e.g., Mertes 1994; Goodbred and Kuehl 1998; Phillips et al. 2004), paraglacial landscapes offer additional sediment sinks along their transport pathways. For example, the Connecticut River (USA) contains off-river water bodies that trap sediments through tidal pumping (Woodruff et al. 2013; Yellen et al. 2017). Large lakes also trap sediment in the upper watersheds of many New England rivers (Meade 1982; Caldwell et al. 1989). In fact, some sediment in paraglacial landscapes may never reach a large river because of natural sediment trapping in ponds and on low-relief coastal plains (Kasprak et al. 2013). Additionally, in New England and other areas with European-style agriculture, sediment may accumulate behind mill dams and on the upslope side of stone walls built by early Colonial farmers (Walter and Merritts 2008; Johnson and Ouimet 2016; Johnson et al. 2018), further preventing sediment from reaching the coast.

Concurrent with extensive upstream land clearing in the White Mountains of New Hampshire during the mid-19th century was downstream dam building within the lower Merrimack River (Fig. 2). Such dams can greatly reduce sediment loads: globally, these have caused a ~20% decrease in sediment discharge (e.g., Syvitski et al. 2005; Gupta et al. 2012). Regionally, Weston (2014) found a correlation between water storage behind dams and decreased fluvial suspended sediment concentrations within U.S. Atlantic and Gulf coast rivers. For example, examination of the Merrimack Village Dam, one of the nearly 850 small "run-of-the-river" dams in the Merrimack River watershed (American Rivers 2016), revealed that it had captured ~62 000 m^3 of sediment between 1734 CE and its removal in 2008 CE (Pearson et al. 2011), the equivalent of ~1.5 years of bedload export from the Merrimack River (41 600 m^3/year; Hein et al. 2014). Hence, it is probable that the largest volume of eroded sediment within the Merrimack River watershed was (and, therefore largely remains) trapped behind 19th century industrial dams, moderating estuarine sediment fluxes during a time of otherwise enhanced terrestrial sediment production. These studies reveal the relatively delayed and complex response of coastal sediment fluxes to time-varying land-use changes across different parts of the watershed over the course of >150 years.

6. Conclusions

This study uses historical, sedimentological, geochronological, geochemical, and palynological data from the paraglacial Merrimack River estuary to reconstruct patterns of pre- and post-European Colonial sedimentation. These data reveal changes in both the rate and source of estuarine sedimentation that are influenced by a range of local- and regional-scale factors related to land-use change and environmental conditions. Sediment accumulation rates in the Merrimack River estuary increased by an order of magnitude following European-style land clearing during the 17th and 18th centuries, but the overall increase in terrestrially derived sediment to the estuary may have been tempered by estuarine equilibrium dynamics as well as sediment trapping on the terrestrial landscape and behind dams. In particular, our data indicate that the Merrimack River watershed responded to land-use changes in a nonuniform manner, likely reflecting long periods of land-use change as settlement gradually impacted regions further upstream in the drainage basin. For example, industrial dams constructed in the lower reaches of the Merrimack Valley (mid-1800s CE) may trap sediments derived from extensive upstream deforestation (late-1800s CE). Additionally, local estuarine processes, such as tidal channel migration

and subsequent infilling have complicated the estuarine sedimentary records obtained from Joppa Flats, which highlights the importance of using multidisciplinary approaches and multi-proxy records to interpret and document changes within coupled human–natural systems.

Acknowledgements

We greatly appreciate the thoughtful and constructive reviews of this manuscript by Gary Mahon, Steven Gray, and Christopher Swezey of the U.S. Geological Survey (USGS), Associate Editor Eli Lazarus, and two anonymous reviewers. We thank Z. Stromer and J. Woodruff for assistance in the field, A. Fallon and C. Shuman for assistance in both the field and laboratory, K. Swanger for logistical support, and T. Sheehan and D. Carriker for laboratory preparation of palynological samples. This research was funded by the National Science Foundation Coastal SEES (award No. OCE 1325430), the Charles Center at William & Mary, and the Southeastern Section of the Geological Society of America. The Virginia Institute of Marine Science (VIMS) National Science Foundation REU Program (award No. OCE 1062882) and a VIMS Short Trust GK-12 Fellowship supported JLS. The USGS Land Change Science Program supported DAW. JLS, CJH, and EAC posed the questions and designed the research. JLS and CJH were responsible for most data collection and laboratory processing, with significant contributions from JMK for radioisotope geochronology, DAW for palynology, GGF for historical and archival research, and IYG for hydrodynamic simulations. All authors were involved in data analysis and interpretation. JLS wrote the paper with significant contributions from all authors. We acknowledge the sampling permissions provided by the Newburyport Conservation Commission. This paper is contribution No. 3852 of the Virginia Institute of Marine Science, William & Mary. Any use of trade, firm, or product names is for descriptive purposes only and does not imply endorsement by the U.S. Government.

References

American Rivers. 2016. Merrimack River. *In* America's most endangered rivers 2016. Available from https://s3.amazonaws.com/american-rivers-website/wp-content/uploads/2016/02/20135708/MER2016_FullReport.pdf.

Andersen, T.J., Mikkelsen, O.A., and Møller, A.L. Morten Pejrup. 2000. Deposition and mixing depths on some European intertidal mudflats based on ^{210}Pb and ^{137}Cs activities. Cont. Shelf Res. **20**(12–13): 1569–1591. doi: 10.1016/S0278-4343(00)00038-8.

Appleby, P.G. 2001. Chronostratigraphic techniques in recent sediments. *In* Tracking environmental change using lake sediments. Volume 1: Basin analysis, coring, and chronological techniques. *Edited by* W.M. Last and J.P. Smol. Springer Netherlands, the Netherlands. pp. 171–203.

Appleby, P.G., and Oldfield, F. 1978. The calculation of lead-210 dates assuming a constant rate of supply of unsupported ^{210}Pb to the sediment. CATENA, **5**(1): 1–8. doi: 10.1016/S0341-8162(78)80002-2.

Bianchi, T.S., and Bauer, J.E. 2011. Particulate organic carbon cycling and transformation. *In* Treatise on estuarine and coastal science. Elsevier. pp. 69–117. doi: 10.1016/B978-0-12-374711-2.00503-9.

Blaauw, M. 2010. Methods and code for 'classical' age-modelling of radiocarbon sequences. Quat. Geochronol. **5**(5): 512–518. doi: 10.1016/j.quageo.2010.01.002.

Bradlee, F.B.C. 1920. Some account of steam navigation in New England. Essex institute. Available from http://books.google.com/books?id=GbQZAAAAYAAJ.

Bronk Ramsey, C. 2009. Bayesian analysis of radiocarbon dates. Radiocarbon, **51**(1): 337–360. doi: 10.1017/S0033822200033865.

Caldwell, D.W., FitzGerald, D.M., and Fenster, M.S. 1989. Origin and sedimentation of Maine lakes with emphasis on lake-outlet deltas. *In* Studies in Maine geology. *Edited by* R.D. Tucker and R.G. Marvinney. Department of Conservation, Maine Geological Survey, Augusta, Georgia. pp. 97–108.

Carey, J.C., Moran, S.B., Kelly, R.P., Kolker, A.S., and Fulweiler, R.W. 2017. The declining role of organic matter in New England salt marshes. Estuaries Coasts, **40**(3): 626–639. doi: 10.1007/s12237-015-9971-1.

Cloern, J.E., Canuel, E. A., and Harris, D. 2002. Stable carbon and nitrogen isotope composition of aquatic and terrestrial plants of the San Francisco Bay estuarine system. Limnol. Oceanogr. **47**(3): 713–729. doi: 10.4319/lo.2002.47.3.0713.

Currier, J.J. 1902. History of Newbury, Mass. 1635–1902. Damrell & Upham, Boston, Mass. Available from https://archive.org/details/historyofnewbury1902curr.

Currin, C.A., Newell, S.Y., and Paerl, H.W. 1995. The role of standing dead Spartina alterniflora and benthic microalgae in salt marsh food webs: Considerations based on multiple stable isotope Analysis. Mar. Ecol. Prog. Ser. **121**: 99–116. doi: 10.3354/meps121099.

Davis, R.B., Hess, C.T., Norton, S.A., Hanson, D.W., Hoagland, K.D., and Anderson, D.S. 1984. ^{137}Cs and ^{210}Pb dating of sediments from soft-water lakes in New England (U.S.A.) and Scandinavia, a failure of ^{137}Cs dating. Chem. Geol. **44**(1–3): 151–185. doi: 10.1016/0009-2541(84)90071-8.

Defina, A., Carniello, L., Fagherazzi, S., and D'Alpaos, L. 2007. Self-organization of shallow basins in tidal flats and salt marshes. J. Geophys. Res. Earth Surf. **112**(3): 1–11. doi: 10.1029/2006JF000550.

Donahue, B. 2004. The great meadow: Farmers and land in colonial Concord. Yale University Press, New Haven, Conn.

Elliott, E.A., McKee, B.A., and Rodriguez, A.B. 2015. The utility of estuarine settling basins for constructing multi-decadal, high-resolution records of sedimentation. Estuar. Coast. Shelf Sci. **164**: 105–114. doi: 10.1016/j.ecss.2015.06.002.

Fagherazzi, S., Carniello, L., D'Alpaos, L., and Defina, A. 2006. Critical bifurcation of shallow microtidal landforms in tidal flats and salt marshes. Proc. Natl. Acad. Sci. **103**(22): 8337–8341. doi: 10.1073/pnas.0508379103. PMID: 16707583.

Fagherazzi, S., Palermo, C., Rulli, M.C., Carniello, L., and Defina, A. 2007. Wind waves in shallow microtidal basins and the dynamic equilibrium of tidal flats. J. Geophys. Res. Earth Surf. **112**(2): 1–12. doi: 10.1029/2006JF000572.

Fallon, A.R., Hoagland, P., Jin, D., Phalen, W., Fitzsimons, G.G., and Hein, C.J. 2017. Adapting without retreating: Responses to shoreline change on an inlet-associated coastal beach. Coast. Manage. **45**(5): 360–383. doi: 10.1080/08920753.2017.1345607.

FitzGerald, D.M., Rosen, P.S., and van Heteren, S. 1994. New England barriers. *In* Geology of Holocene barrier island systems. *Edited by* R.A. Davis. Springer-Verlag, Berlin, Germany. doi: 10.1007/978-3-642-78360-9.

FitzGerald, D.M., Buynevich, I.V., Fenster, M.S., Kelley, J.T., and Belknap, D.F. 2005. Coarse-grained sediment transport in northern New England estuaries — A synthesis. *In* High resolution morphodynamics and sedimentary evolution of estuaries, 8th edition. *Edited by* D.M. FitzGerald and J. Knight. Springer Netherlands, the Netherlands. pp. 195–213.

Flanagan, S.M., Nielsen, M.G., Robinson, K.W., and Coles, J.F. 1999. Water-quality assessment of the New England Coastal Basins in Maine, Massachusetts, New Hampshire, and Rhode Island: environmental settings and implications for water quality and aquatic biota. doi: 10.3133/wri984249.

Forbes, D.L., and Syvitski, J.P.M. 1994. Paraglacial coasts. *In* Coastal evolution: Late quaternary shoreline morphodynamics. *Edited by* R.W.G. Carter and C.D. Woodroffe. Cambridge University Press, Cambridge. pp. 373–424.

Foster, D.R. 1992. Land-use history (1730-1990) and vegetation dynamics in central New England, USA. J. Ecol. **80**(4): 753–772. Available from http://www.jstor.org/stable/2260864. doi: 10.2307/2260864.

Francis, D.R., and Foster, D.R. 2001. Response of small New England ponds to historic land use. Holocene, **11**(3): 301–312. doi: 10.1191/095968301666282469.

Fruergaard, M., Andersen, T.J., Nielsen, L.H., Madsen, A.T., Johannessen, P.N., Murray, A.S., et al. 2011. Punctuated sediment record resulting from channel migration in a shallow sand-dominated micro-tidal lagoon, Northern Wadden Sea, Denmark. Mar. Geol. **280**(1–4): 91–104. doi: 10.1016/j.margeo.2010.12.003.

Fry, B., and Sherr, E.B. 1984. δ^{13}C measurements as indicators of carbon flow in marine and freshwater ecosystems. Contrib. Mar. Sci. **27**: 13–47. Available from https://repositories.lib.utexas.edu/handle/2152/18034.

Goodbred, S.L., and Kuehl, S.A. 1998. Floodplain processes in the Bengal Basin and the storage of Ganges-Brahmaputra river sediment: An accretion study using ^{137}Cs and ^{210}Pb geochronology. Sediment. Geol. **121**(3–4): 239–258. doi: 10.1016/S0037-0738(98)00082-7.

Gupta, H., Kao, S.J., and Dai, M. 2012. The role of mega dams in reducing sediment fluxes: A case study of large Asian rivers. J. Hydrol. **464**–**465**: 447–458. doi: 10.1016/j.jhydrol.2012.07.038.

Hanson, L.S., and Caldwell, D.W. 1989. The lithologic and structural controls on the geomorphology of the mountainous areas in north-central Maine. *In* Studies in Maine geology. *Edited by* R.D. Tucker and R.G. Marvinney. Department of Conservation, Maine Geological Survey, Augusta, Georgia. pp. 147–167.

Hartwell, A.D. 1970. Hydrography and Holocene sedimentation of the Merrimack River estuary Massachusetts. *In* Contribution no. 5-CRG obtained under contract no. NR N0014-67-A-0230-0001, task order no. NR 3888-844 of the Geography Brach, Office of Naval Research.

Hedges, J.I., and Keil, R.G. 1995. Sedimentary organic matter preservation: an assessment and speculative synthesis. Mar. Chem. **49**(2–3): 81–115. doi: 10.1016/0304-4203(95)00008-F.

Hein, C.J., FitzGerald, D.M., Carruthers, E.A., Stone, B.D., Barnhardt, W.A., and Gontz, A.M. 2012. Refining the model of barrier island formation along a paraglacial coast in the Gulf of Maine. Mar. Geol. **307**–**310**: 40–57. doi: 10.1016/j.margeo.2012.03.001.

Hein, C.J., FitzGerald, D.M., Buynevich, I.V., Heteren, S.V.A.N., and Kelley, J.T. 2014. Evolution of paraglacial coasts in response to changes in fluvial sediment supply. Geol. Soc. London, Spec. Publ. **388**: 247–280. doi: 10.1144/SP388.15.

Hein, C.J., Fallon, A.R., Rosen, P., Hoagland, P., Georgiou, I.P., Fitzgerald, D., et al. 2019. Shoreline dynamics along a developed river mouth barrier island: Multi-decadal cycles of erosion and event-driven mitigation. Front. Earth Sci. **7**: 1–23. doi: 10.3389/feart.2019.00103.

Hopkinson, C.S., Morris, J.T., Fagherazzi, S., Wollheim, W.M., and Raymond, P.A. 2018. Lateral marsh edge erosion as a source of sediments for vertical marsh accretion. J. Geophys. Res. Biogeosci. doi: 10.1029/2017JG004358.

Hu, Z., van der Wal, D., Cai, H., van Belzen, J., and Bouma, T.J. 2018. Dynamic equilibrium behaviour observed on two contrasting tidal flats from daily monitoring of bed-level changes. Geomorphology, **311**: 114–126. doi: 10.1016/j.geomorph.2018.03.025.

Hubeny, J.B., Kristiansen, E., Danikas, A., Zhu, J., McCarthy, F.M.G., Cantwell, M.G., et al. 2018. Multi-century record of anthropogenic impacts on an urbanized mesotidal estuary: Salem Sound, MA. Estuaries Coasts, **41**(2): 404–420. doi: 10.1007/s12237-017-0298-y.

Jalowska, A.M., Rodriguez, A.B., and McKee, B.A. 2015. Responses of the Roanoke bayhead delta to variations in sea level rise and sediment supply during the Holocene and Anthropocene. Anthropocene, **9**: 41–55. doi: 10.1016/j.ancene.2015.05.002.

Johnson, K.M., and Ouimet, W.B. 2016. Physical properties and spatial controls of stone walls in the northeastern USA: Implications for Anthropocene studies of 17th to early 20th century agriculture. Anthropocene, **15**: 22–36. doi: 10.1016/j.ancene.2016.07.001.

Johnson, K.M., Snyder, N.P., Castle, S., Hopkins, A.J., Waltner, M., Merritts, D.J., et al. 2018. Legacy sediment storage in New England river valleys: Anthropogenic processes in a postglacial landscape. Geomorphology, **327**: 417–437. doi: 10.1016/j.geomorph.2018.11.017.

Kasprak, A., Magilligan, F.J., Nislow, K.H., Renshaw, C.E., Snyder, N.P., and Dade, W.B. 2013. Differentiating the relative importance of land cover change and geomorphic processes on fine sediment sequestration in a logged watershed. Geomorphology, **185**: 67–77. doi: 10.1016/j.geomorph.2012.12.005.

Kemp, A.C., Sommerfield, C.K., Vane, C.H., Horton, B.P., Chenery, S., Anisfeld, S., et al. 2012. Use of lead isotopes for developing chronologies in recent salt-marsh sediments. Quat. Geochronol. **12**: 40–49. doi: 10.1016/j.quageo.2012.05.004.

Kirwan, M.L., Murray, A.B., Donnelly, J.P., and Corbett, D.R. 2011. Rapid wetland expansion during European settlement and its implication for marsh survival under modern sediment delivery rates. Geology, **39**: 507–510. doi: 10.1130/G31789.1.

Labaree, B.W. 1962. Patriots and Partisans: The Merchants of Newburyport, 1764–1815. Harvard University Press, Cambridge, Mass.

Lesser, G.R., Roelvink, D., van Kester, J.A.T.M., and Stelling, G.S. 2004. Development and validation of a three-dimensional morphological model. Coast. Eng. **51**(8–9): 883–915. doi: 10.1016/j.coastaleng.2004.07.014.

Malone, P.M. 2009. Waterpower in Lowell: Engineering and industry in Nineteenth Century America. The Johns Hopkins University Press, Baltimore, Md.

Mattheus, C.R., Rodriguez, A.B., and McKee, B.A. 2009. Direct connectivity between upstream and downstream promotes rapid response of lower coastal-plain rivers to land-use change. Geophys. Res. Lett. **36**(20). doi: 10.1029/2009GL039995.

Mayer, B., Boyer, E.W., Goodale, C., Jaworski, N.A., Van Breemen, N., Howarth, R.W., et al. 2002. Sources of nitrate in rivers draining sixteen watersheds in the northeastern U.S.: Isotopic constraints. Biogeochemistry, **57–58**: 171–197. doi: 10.1023/A:1015744002496.

Meade, R.H. 1969. Landward transport of bottom sediments in estuaries of the Atlantic coastal plain. J. Sediment. Res. **39**(1): 222–234. doi: 10.1306/74D71C1C-2B21-11D7-8648000102C1865D.

Meade, R.H. 1982. Sources, sinks, and storage of river sediment in the Atlantic drainage of the United States. J. Geol. **90**(3): 235–252. doi: 10.1086/628677.

Mertes, L.A.K. 1994. Rates of flood-plain sedimentation on the central Amazon River. Geology, **22**(2): 171. doi: 10.1130/0091-7613(1994)022<0171:ROFPSO>2.3.CO;2.

Molloy, P.M. 1976. The lower Merrimack Valley: An inventory of historic engineering and industrial sites. Merrimack Valley Textile Museum, North Andover, Massachusetts, and Historic American Engineering Record, National Park Service, Washington, D.C.

Munsell. 2000. Munsell soil color charts. GretagMacbeth, New Windsor, N.Y.

Neumeier, U., Ferrarin, C., Amos, C.L., Umgiesser, G., and Li, M.Z. 2008. Sedtrans05: An improved sediment-transport model for continental shelves and coastal waters with a new algorithm for cohesive sediments. Comput. Geosci. **34**(10): 1223–1242. doi: 10.1016/j.cageo.2008.02.007.

Pasternack, G.B., Brush, G.S., and Hilgartner, W.B. 2001. Impact of historic land-use change on sediment delivery to a Chesapeake Bay subestuarine delta. Earth Surf. Process. Landforms **26**: 409–427. doi: 10.1002/esp.189.

Pearson, A.J., Snyder, N.P., and Collins, M.J. 2011. Rates and processes of channel response to dam removal with a sand-filled impoundment. Water Resour. Res. **47**(8): 1–15. doi: 10.1029/2010WR009733.

Phillips, J.D., Slattery, M.C., and Musselman, Z.A. 2004. Dam-to-delta sediment inputs and storage in the lower trinity river, Texas. Geomorphology, **62**(1–2): 17–34. doi: 10.1016/j.geomorph.2004.02.004.

Priestas, A.M., Fagherazzi, S., Wilson, C.A., and FitzGerald, D.M. 2012. Rapid wetland expansion during European settlement and its implication for marsh survival under modern sediment delivery rates: Comment. Geology, **40**(12): e284–e285. doi: 10.1130/G32597C.1.

Ralston, D.K., Geyer, W.R., and Lerczak, J.A. 2010. Structure, variability, and salt flux in a strongly forced salt wedge estuary. J. Geophys. Res. **115**(C6): C06005. doi: 10.1029/2009JC005806.

Reimer, P.J., Bard, E., Bayliss, A., Beck, J.W., Blackwell, P.G., Ramsey, C.B., et al. 2013. IntCal13 and Marine13 radiocarbon age calibration curves 0–50,000 Years cal BP. Radiocarbon, **55**(04): 1869–1887. doi: 10.2458/azu_js_rc.55.16947.

Russell, K.L., Vietz, G.J., and Fletcher, T.D. 2018. Urban catchment runoff increases bedload sediment yield and particle size in stream channels. Anthropocene, **23**: 53–66. doi: 10.1016/j.ancene.2018.09.001.

Saintilan, N., Rogers, K., Mazumder, D., and Woodroffe, C. 2013. Allochthonous and autochthonous contributions to carbon accumulation and carbon store in southeastern Australian coastal wetlands. Estuar. Coast. Shelf Sci. **128**: 84–92. doi: 10.1016/j.ecss.2013.05.010.
Slattery, M.C., and Phillips, J.D. 2011. Controls on sediment delivery in coastal plain rivers. J. Environ. Manage. **92**(2): 284–289. doi: 10.1016/j.jenvman.2009.08.022. PMID: 19892459.
Smith, E.V. 1854. History of Newburyport: From the earliest settlement of the country to the present time. Cornell University Library, Ithaca, N.Y.
Steinberg, T. 1991. Nature incorporated: Industrialization and the waters of New England. Cambridge University Press, Cambridge.
Stone, B., Stone, J., and DiGiacomo-Cohen, M. 2006. Surficial geologic map of the Salem-Newburyport East-Wilmington-Rockport quadrangle area in northeast Massachusetts. US Geological Survey Open-File Report. doi: 10.3133/ofr20061260B.
Syvitski, J.P.M., Vörösmarty, C.J., Kettner, A.J., and Green, P. 2005. Impact of humans on the flux of terrestrial sediment to the global coastal ocean. Science, **308**(5720): 376–380. doi: 10.1126/science.1109454. PMID: 15831750.
Tambroni, N., and Seminara, G. 2006. Are inlets responsible for the morphological degradation of Venice Lagoon? J. Geophys. Res. Earth Surf. **111**(3): 1–19. doi: 10.1029/2005JF000334.
Traverse, A. 2007. Paleopalynology. Springer Netherlands, Dordrecht, the Netherlands.
Tweel, A.W., and Turner, R.E. 2012. Watershed land use and river engineering drive wetland formation and loss in the Mississippi River birdfoot delta. Limnol. Oceanogr. **57**(1): 18–28. doi: 10.4319/lo.2012.57.1.0018.
U.S. Army Corps of Engineers. 1835. Report of Chief Engineer in Message from the President of the United States to the two Houses of Congress, at the commencement of the first session of the twenty-fourth Congress, December 8, 1835.
U.S. Army Corps of Engineers. 1911. Influence of forests on the run-off in the Merrimac River basin: New Hampshire and Massachusetts. 62nd United States Congress, Document Number 9.
U.S. Army Corps of Engineers. 2018. 2014 USACE NAE Topobathy Lidar: Newbury (MA).
Van Der Wal, D., Pye, K., and Neal, A. 2002. Long-term morphological change in the Ribble Estuary, northwest England. Mar. Geol. **189**(3–4): 249–266. doi: 10.1016/S0025-3227(02)00476-0.
Walter, R.C., and Merritts, D.J. 2008. Natural streams and the legacy of water-powered mills. Science, **319**(5861): 299–304. doi: 10.1126/science.1151716. PMID: 18202284.
Ward, L.G., Zaprowski, B.J., Trainer, K.D., and Davis, P.T. 2008. Stratigraphy, pollen history and geochronology of tidal marshes in a Gulf of Maine estuarine system: Climatic and relative sea level impacts. Mar. Geol. **256**(1–4): 1–17. doi: 10.1016/j.margeo.2008.08.004.
Watson, E.B., Raposa, K.B., Carey, J.C., Wigand, C., and Warren, R.S. 2017*a*. Anthropocene survival of southern New England's salt marshes. Estuaries Coasts, **40**(3): 617–625. doi: 10.1007/s12237-016-0166-1.
Watson, E.B., Wigand, C., Davey, E.W., Andrews, H.M., Bishop, J., and Raposa, K.B. 2017*b*. Wetland loss patterns and inundation-productivity relationships prognosticate widespread Salt Marsh Loss for southern New England. Estuaries Coasts, **40**(3): 662–681. doi: 10.1007/s12237-016-0069-1.
Weston, N.B. 2014. Declining sediments and rising seas: An unfortunate convergence for tidal wetlands. Estuaries Coasts, **37**(1): 1–23. doi: 10.1007/s12237-013-9654-8.
Whiteside, J.H., Olsen, P.E., Eglinton, T.I., Cornet, B., McDonald, N.G., and Huber, P. 2011. Pangean great lake paleoecology on the cusp of the end-Triassic extinction. Palaeogeogr. Palaeoclimatol. Palaeoecol. **301**(1–4): 1–17. doi: 10.1016/j.palaeo.2010.11.025.
Willard, D.A., Weimer, L.M., and Riegel, W.L. 2001. Pollen assemblages as paleoenvironmental proxies in the Florida Everglades. Rev. Palaeobot. Palynol. **113**(4): 213–235. doi: 10.1016/S0034-6667(00)00042-7. PMID: 11179714.
Wood, G.K., Swallow, L.A., Johnson, C.G., and Searles, G.H. 1970. Flood of March 1968 in Eastern Massachusetts and Rhode Island. U.S. Geological Survey Report. doi: 10.3133/ofr70373.
Woodruff, J.D., Martini, A.P., Elzidani, E.Z.H.H., Naughton, T.J., Kekacs, D.J., and MacDonald, D.G. 2013. Off-river waterbodies on tidal rivers: Human impact on rates of infilling and the accumulation of pollutants. Geomorphology, **184**: 38–50. doi: 10.1016/j.geomorph.2012.11.012.
Xu, D., Bai, Y., Ji, C., and Williams, J. 2015. Experimental study of the density influence on the incipient motion and erosion modes of muds in unidirectional flows: the case of Huangmaohai Estuary. Ocean Dyn. **65**: 187–201. doi: 10.1007/s10236-014-0803-9.
Yellen, B., Woodruff, J.D., Ralston, D.K., MacDonald, D.G., and Jones, D.S. 2017. Salt wedge dynamics lead to enhanced sediment trapping within side embayments in high-energy estuaries. J. Geophys. Res. Ocean. **122**(3): 2226–2242. doi: 10.1002/2016JC012595.
Zimmerman, A.R., and Canuel, E.A. 2000. A geochemical record of eutrophication and anoxia in Chesapeake Bay sediments: Anthropogenic influence on organic matter composition. Mar. Chem. **69**(1–2): 117–137. doi: 10.1016/S0304-4203(99)00100-0.
Zimmerman, A.R., and Canuel, E.A. 2002. Sediment geochemical records of eutrophication in the mesohaline Chesapeake Bay. Limnol. Oceanogr. **47**(4): 1084–1093. doi: 10.4319/lo.2002.47.4.1084.